J|A|C|S
ARTICLES
Published on Web 03/09/2007

Quasi Chiral Phase Separation in a Two-Dimensional Orientationally Disordered System: 6-Nitrospiropyran on Au(111)

Tian Huang, Zhenpeng Hu, Aidi Zhao, Haiqian Wang, Bing Wang, Jinlong Yang, and J. G. Hou*

Contribution from the Hefei National Laboratory for Physical Sciences at Microscale, University of Science and Technology of China, Hefei, Anhui 230026, People's Republic of China

Received September 9, 2006; E-mail: jghou@ustc.edu.cn

Abstract: The adsorption and chiral expression of 6-nitrospiropyran (SP6) molecules on a Au(111) surface are studied by scanning tunneling microscopy (STM) in combination with density functional theory (DFT) calculations. Both the chirality and the adsorption orientation of each adsorbed SP6 molecule are determined. The racemic mixture of SP6 enantiomers forms two-dimensional (2D) domains with same close packed positional orders but different internal orientational structures due to the random distribution of two adsorption orientations in each domain. However, all these orientationally disordered 2D domains undergo spontaneous quasi chiral phase separation; the 2D SP6 domains separate into 1D homochiral chains in which the SP6 molecules adopt two orientations randomly. This novel phenomenon is attributed to the preferential formation of the energetic favorable configurations with both the C−H···O weak hydrogen bonds and the π-stacking of the two moieties of each SP6 molecule.

Introduction

The chiral chemistry in two-dimensional (2D) molecules/substrate systems is of both technological and fundamental importance and has attracted numerous interests in the past decade.[1−5] Constructing a chiral surface is a crucial step for enantioselective heterogeneous catalysis in chemical and pharmaceutical industries.[6−10] On the other hand the fundamental investigation of molecular chirality is more feasible in 2D systems due to the reduction of the spatial freedom. With the help of scanning tunneling microscopy (STM), various chiral phenomena such as chiral resolution,[11−22] chirality amplification,[23] chiral phase transition,[11,12,24] and loss of chirality[25] have been directly observed at the submolecular scale in 2D molecules/substrate systems.

Spontaneous resolution, i.e., the chiral separation of the racemic mixture into enantiomorphic condensates upon crystallization, is an intriguing and valuable chiral phenomenon which has been observed in various media such as crystals,[26] liquid crystals,[27] self-assembled helical fibers,[28] and 2D molecules/substrate systems.[11−22] Previous STM observations revealed that both prochiral[10−14] and chiral[15−22] molecules could undergo spontaneous resolution upon adsorption on surfaces. The enantiomorphic condensates that resulted from the segregations included 2D domains,[10,11,15−18] 1D molecular chains,[12−14,18−20] and 0D molecular clusters.[14,21,22] But the STM investigations

(1) Jannes, G., Dubois, V., Eds. *Chiral Reactions in Heterogeneous Catalysis*; Plenum: New York, 1995.
(2) Baiker, A.; Blaser, H. U. In *Handbook of Heterogeneous Catalysis*; Ertl, G., Knözinger, H., Weitkamp, J., Eds.; VCH: Weinheim, 1997; Vol. 5, pp 2422−2430.
(3) Baddeley, C. J. *Top. Catal.* **2003**, *25*, 17−28.
(4) Verbiest, T.; Elshocht, S. V.; Kauranen, M.; Hellemans, L.; Snauwaert, J.; Nuckolls, C.; Katz, T. J.; Persoons, A. *Science* **1998**, *282*, 931−915.
(5) Bodenhöfer, K.; Hierlemann, A.; Seemann, J.; Gauglitz, G.; Koppenhoefer, B.; Göpel, W. *Nature* **1997**, *387*, 577−580.
(6) Ohtani, B.; Shintani, A.; Uosaki, K. *J. Am. Chem. Soc.* **1999**, *121*, 6515−6516.
(7) Zhao, X. *J. Am. Chem. Soc.* **2000**, *122*, 12584−12585.
(8) Lorenzo, M.; Baddeley, C.; Muryn, C.; Raval, R. *Nature* **2000**, *404* (6776), 376−379.
(9) Schunack, M.; Lægsgaard, E.; Stensgaard, I.; Johannsen, I.; Besenbacher, F. *Angew. Chem., Int. Ed.* **2001**, *40*, 2623−2626.
(10) France, C.; Parkinson, B. *J. Am. Chem. Soc.* **2003**, *125*, 12712−12713.
(11) Vidal, F.; Delvigne, E.; Stepanow, S.; Lin, N.; Barth, J. V.; Kern, K. *J. Am. Chem. Soc.* **2005**, *127*, 10101−10106.
(12) Böhringer, M.; Schneider, W.-D.; Berndt, R. *Angew. Chem., Int. Ed.* **2000**, *39*, 792−795.
(13) Barth, J. V.; Weckesser, J.; Trimarchi, G.; Vladimirova, M.; De Vita, A.; Cai, C.; Brune, H.; Günter, P.; Kern, K. *J. Am. Chem. Soc.* **2002**, *124*, 7991−8000.
(14) Böhringer, M.; Morgenstern, K.; Schneider, W.-D.; Berndt, R.; Mauri, F.; De Vita, A.; Car, R. *Phys. Rev. Lett.* **1999**, *83*, 324−327.
(15) Fang, H. B.; Giancarlo, L. C.; Flynn, G. W. *J. Phys. Chem. B* **1998**, *102* (38), 7311−7315.
(16) Xu, Q. M.; Wang, D.; Wan, L. J.; Wang, C.; Bai, C. L.; Feng, G. Q.; Wang, M. X. *Angew. Chem., Int. Ed.* **2002**, *41*, 3408−3411.
(17) Fasel, R.; Parschau, M.; Ernst, K.-H. *Angew. Chem., Int. Ed.* **2003**, *42*, 5178−5181.
(18) De Feyter, S.; Gesquière, A.; Wurst, K.; Amabilino, D. B.; Veciana, J.; De Schryver, F. C. *Angew. Chem., Int. Ed.* **2001**, *40*, 3217−3220.
(19) Cai, Y.; Bernasek, S. L. *J. Am. Chem. Soc.* **2003**, *125*, 1655−1659.
(20) Cai, Y.; Bernasek, S. L. *J. Phys. Chem. B* **2005**, *109*, 4514−4519.
(21) Kühnle, A.; Linderoth, T. R.; Hammer, B.; Besenbacher, F. *Nature* **2002**, *415*, 891−893.
(22) Blüm, M.-C.; Cavar, E.; Pivetta, M.; Patthey, F.; Schneider, W.-D. *Angew. Chem., Int. Ed.* **2005**, *44*, 5334−5337.
(23) Fasel, R.; Parschau, M.; Ernst, K.-H. *Nature* **2006**, *439*, 449−452.
(24) Weigelt, S.; Busse, C.; Petersen, L.; Rauls, E.; Hammer, B.; Gothelf, K.; Besenbacher, F.; Linderoth, T. *Nat. Mater.* **2006**, *5*, 112−117.
(25) Zhang, J.; Gesquière, A.; Sieffert, M.; Klapper, M.; Müllen, K.; De Schryver, F. C.; De Feyter, S. *Nano. Lett.* **2005**, *5*, 1395−1398.
(26) Pasteur, L. *Ann. Phys.* **1848**, *24*, 442.
(27) Takanishi, Y.; Takezoe, H.; Suzuki, Y.; Kobayashi, I.; Yajima, T.; Terada, M.; Mikami, K. *Angew. Chem., Int. Ed.* **1999**, *38*, 2354−2356.
(28) Sakurai, S.; Okoshi, K.; Kumaki, J.; Yashima, E. *J. Am. Chem. Soc.* **2006**, *128*, 5650−5651.

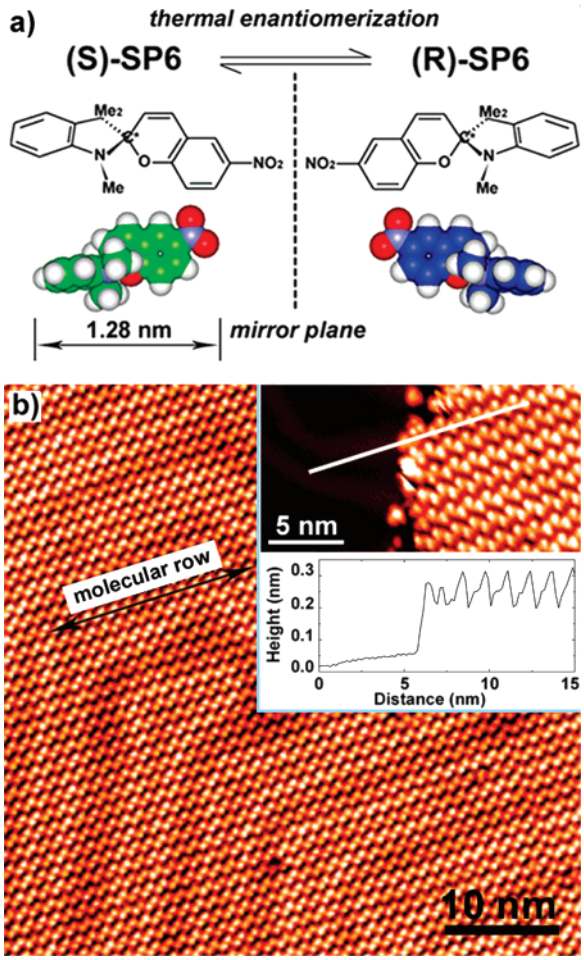

Figure 1. (a) Molecular structures and optimized CPK models of (S)-SP6 and (R)-SP6. (b) Typical STM image (46 × 46 nm^2) of a highly ordered SP6 monolayer on Au(111) surface. Black arrow indicates a molecular row in the 2D SP6 domain. Inset: An area near the edge of the SP6 island displaying both the SP6 domain and bare Au(111) surface. A line profile along the white line gives the apparent height of the SP6 island of ~0.32 nm above the Au(111) surface plane. The sample bias $V_s = +1.8$ V and the tunneling current $I_t = 50$ pA.

of spontaneous resolution of 3D chiral molecules on surfaces are still limited, possibly because the complex 3D shapes of chiral molecules hinder the formation of ordered structures on surfaces and the direct chirality discrimination of the adsorbate is hard to achieve.

In this work we report the chiral expression of a racemic mixture of 6-nitrospiropyran (SP6) molecules on Au(111) surfaces. The SP6 enantiomers form large 2D domains with ordered structures in spite of their nonplanar low-symmetry shapes. The remarkable conformity between high-resolution experimental and simulated STM images allows us to identify the adsorption orientation and the absolute chirality of each molecule in the 2D monolayers simultaneously. We find that the random distribution of two adsorption orientations of SP6 leads to diverse 2D domains with identical close packed positional order but different local orientational structures. However, a spontaneous quasi chiral separation[19] can be found in all these structures. To our knowledge, this is the first observation which reveals that the chiral order can exist independently without the presence of orientational order in a 2D molecules/substrate system.

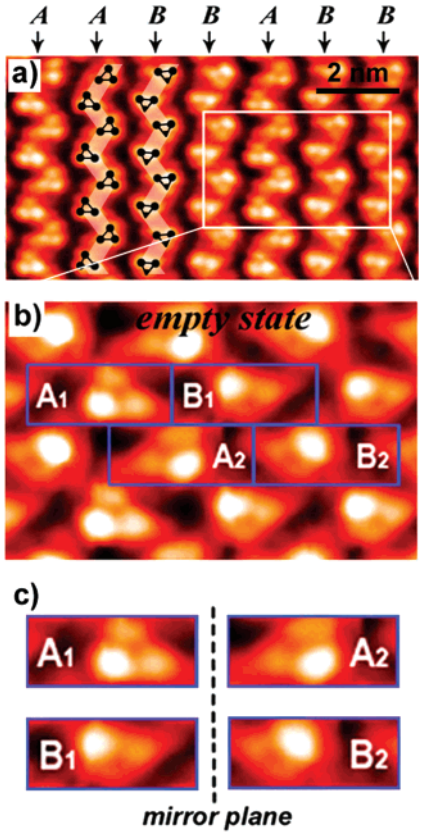

Figure 2. (a) A high-resolution empty state STM image (10 × 5.5 nm^2) revealing the internal patterns of SP6 molecules. A and B indicate two types of molecular rows with different intrarow patterns. Two schematic models were superposed on the STM image in order to facilitate the distinguishing of A- and B-type rows. (b) Higher magnified images of the selected area in (a); four different intramolecular patterns denoted as A_1, A_2, B_1, and B_2 can be found in the image. (c) Four STM patterns extracted from (b). A_1 and A_2 appear as mirror images of each other and so do B_1 and B_2. The sample bias $V_s = +1.8$ V and the tunneling current $I_t = 50$ pA.

Experimental Section

The epitaxial Au(111) substrates with well-defined terraces and single atomic steps on mica were prepared by vacuum deposition.[29] Ar^+ ion sputtering and annealing (to 600 K) cycles were used to clean and flatten the Au(111) surface in the preparation chamber of an Omicron ultrahigh vacuum (UHV) LT-STM system. An SP6 molecule consists of two halves of near-planar heterocyclic fused rings (substituted indoline and chromene) connected at an sp^3 hybrid carbon atom, as shown in Figure 1a. In solid-state SP6, due to the very small thermal barrier, left- (S) and right-handed (R) SP6 molecules interconvert to each other spontaneously at room temperature, thereby forming a natural racemic mixture.[30,31] SP6 in powder form (98%) purchased from Aldrich Co. was degassed in a quartz crucible for more than 24 h and then vapor deposited onto Au(111) at ~350 K. During the deposition process the substrate was held at room temperature and the base pressure was about 3×10^{-6} Pa. The as-deposited sample was transferred from the preparation chamber to the STM chamber (base pressure $<1.0 \times 10^{-8}$ Pa) and cooled down to 78 K for data acquisition. Constant current STM images were recorded with an electrochemically etched tungsten tip, which was subjected to a careful cleaning treatment in advance.

(29) Zeng, C. G.; Wang, H. Q.; Wang, B.; Yang, J. L.; Hou, J. G. *Appl. Phys. Lett.* **2000**, *77*, 3595−3597.
(30) Kiesswetter, R.; Pustet, N.; Brandl, F.; Mannschreck, A. *Tetrahedron: Asymmetry* **1999**, *10*, 4677−4687.
(31) Mannschreck, A.; Lorenz, K.; Schinabeck, M. In *Organic Photochromic and Thermochromic Compounds*; Crano, J. C., Guglielmetti, R., Eds. The enantiomers of 2-donor-substituted benzopyrans and benzo-1,4-oxazines and their thermal racemization. Plenum Press: New York 1999; Vol. 2, pp 261−295.

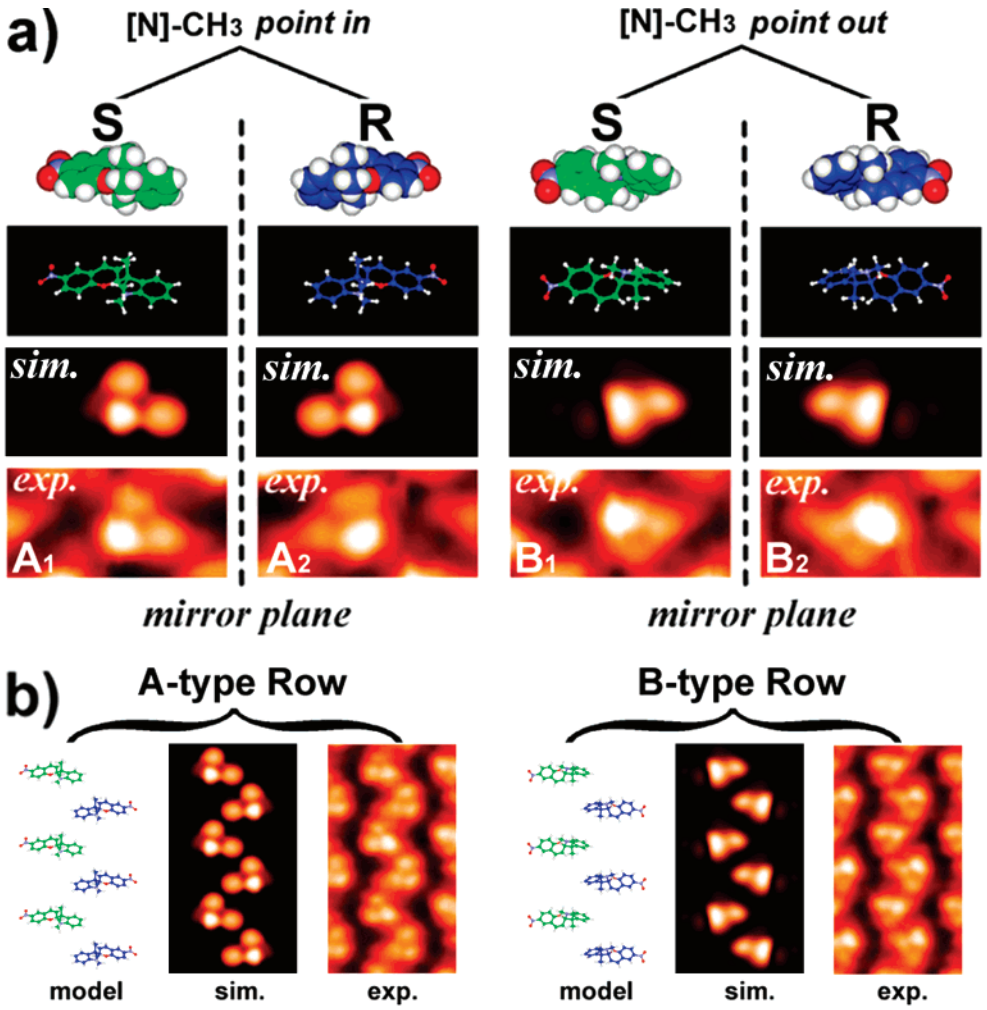

Figure 3. (a) Simulated empty-state images and related top view molecular models of free SP6 molecules (from top to bottom: CPK models, stick models, simulated images, and experimental images). The simulated patterns coincide with the experimental patterns A_1, A_2, B_1, and B_2 quite well. (b) Molecular models, simulated and the experimental images of A- and B-type rows. The experimental STM patterns are extracted from Figure 2.

Results and Discussion

SP6 forms ordered 2D domains composed of parallel molecular rows after vapor deposition onto the Au(111) surface, as shown in Figure 1b. The incommensurate character of the SP6 domains (i.e., there is no distinctive registry between the SP6 lattice and the Au(111) lattice), together with the fact that the reconstruction features of Au(111) can be still seen through the molecular layers, suggests the weak interactions between SP6 and the substrate.[10] We thus consider that the 2D SP6 structures are dominated by the adsorbate−adsorbate interactions rather than the adsorbate−substrate interactions. A line profile (inset of Figure 1b) crossing the SP6 island and the bare Au(111) surface gives the apparent height of the SP6 adlayer of about 0.32 nm, which is much smaller than the length of the molecule, indicating that the SP6 molecules adopt the *flat-lying* rather than the *standing-up* adsorption geometries in the 2D domain.

Figure 2a shows an STM image recorded at a sample bias of +1.8 V, which reveals the empty-state intramolecular patterns of adsorbed SP6 molecules. Each molecule within the SP6 rows is now resolved into triangular geometry with fine structures. According to the directions and the fine structures of the triangles, the parallel rows can be classified into two types designated as A- and B-type respectively in Figure 2a. In detail, the bottom sides of the triangles are nearly horizontal and each triangle appears as three lobes with distinct nodes in the A-type row, while the top sides of the triangles are nearly horizontal and each triangle is composed of an asymmetric *dumb-bell* side and a very weak apex in the B-type row. In addition, a small scale high-resolution empty-state image (Figure 2b) shows the locations of the brightest lobe in the triangles within a single row are different. Thus we finally find four different triangular patterns in the 2D SP6 domain designated as A_1, A_2, B_1, and B_2 in Figure 2b, respectively. More interestingly, we notice that A_1 and A_2 are mirror images of each other and so are B_1 and B_2, as shown in Figure 2c.

It is believed that different intramolecular patterns result from different orientations of two SP6 enantiomers. Once we identify the adsorption orientation and the absolute chirality of each SP6, we will be able to monitor the chiral expression and to investigate the intermolecular interactions involved in the chirality recognition process. However, this task is hard to accomplish only from the STM images, since the STM patterns are not directly related to the geometric aspects but to the electronic structures of the adsorbates. Our previous works revealed that the direct identification of the orientations of adsorbates can be achieved by comparing experimental STM images with simulated ones.[32,33,34] So we conducted a theoretical

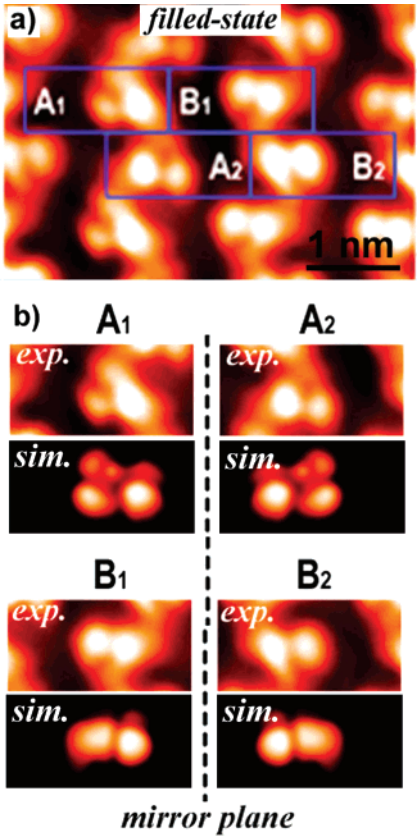

Figure 4. (a) High-resolution filled-state STM images of the same area as Figure 2b. Four different intramolecular patterns can be found, denoted as A_1, A_2, B_1, and B_2. (b) Four different intramolecular patterns together with the most consistent simulated STM images. The sample bias $V_s = -1.6$ V and the tunneling current $I_t = 50$ pA.

STM image simulation of individual (S)- and (R)-SP6 molecules using the density functional theory (DFT) with local density approximation (LDA) implemented. Simulated STM patterns were obtained by integrating the electron density of states (DOS) on a free SP6 from the Fermi level to the bias voltage using the Tersoff−Hamann model.[35,36] Because SP6 is a nonplanar molecule, the 3D molecular structure will affect the tip's track markedly in the scanning process, resulting in the deviation of the experimental STM image from the ideal distribution of the molecular DOS. We take this factor into account by multiplying the DOS with a convolution function in the simulation. To determine the orientations corresponding to the experimental patterns, we rotated an SP6 molecule around the two orthogonal axes in the substrate plane with an angle step of 10° and then compared the simulated STM image of each orientation with the experimental results. Once we found the matched simulated image, a further fine adjustment with the precision of 1° was done until the best agreement between the simulated image and experimental result was obtained.

Figures 3 and 4 show the experimental intramolecular patterns (A_1, A_2, B_1, and B_2) together with the most consistent simulated STM images of the empty and filled states, respectively. Chiral discrimination and orientation identification are achieved simultaneously due to the remarkable conformity between simulated and experimental results. We may find that A_1 and A_2, referring to an (S)-SP6 and an (R)-SP6 respectively, both adopt the *nitrogen atom connected methyl group* ([N]−CH_3) "point-in" adsorption orientation;[37] while B_1 and B_2, referring to an (S)-SP6 and a (R)-SP6 respectively, both adopt the [N]−CH_3

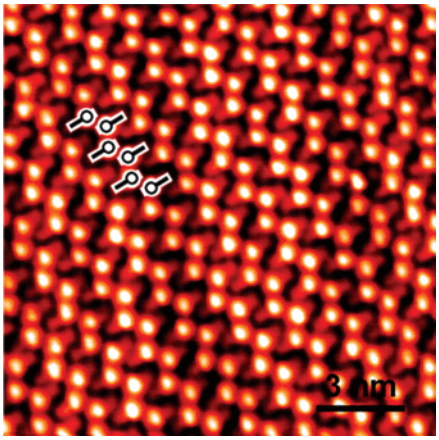

Figure 5. STM image recorded under special tip conditions where the geometric shapes of SP6 molecules were rendered. The superposed schematic models indicate the shapes and arrangements of SP6 molecules within a molecular row. Each SP6 molecule appears as a *pollywog* with a length of ~1.3 nm, and the long axis of each SP6 molecule is nearly perpendicular to the direction of the rows. The combining configurations between adjacent rows are also resolved clearly in this image: Adjacent rows join together just like *zippers* to form the close packed 2D structure. The sample bias $V_s = -1.5$ V and the tunneling current $I_t = 50$ pA.

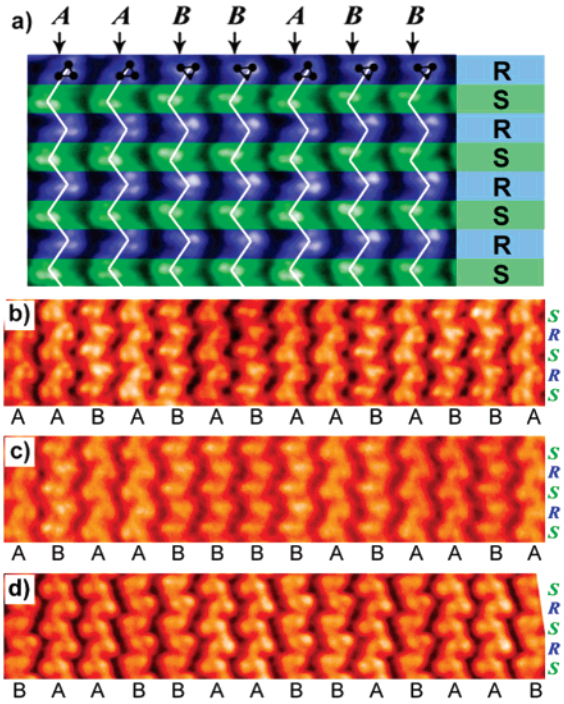

Figure 6. (a) Recolored Figure 2a showing the quasi chiral separation character in the 2D domain. Left- (S) and right-handed (R) chains are colored green and blue, respectively. (b−d) STM images on three different samples. These areas have similar close packed positional order but different local orientational structures due to the irregular distribution of A- and B-type rows along the horizontal direction, as indicated with the letters below each STM image. Nevertheless, these domains all exhibit the quasi chiral separation behavior. The tunneling conditions are sample bias $V_s = -1.8$ V and the tunneling current $I_t = 50$ pA for (b−d).

(32) Hou, J. G.; Yang, J. L.; Wang, H. Q.; Li, Q. X.; Zeng, C. G.; Lin, H.; Wang, B.; Chen, D. M.; Zhu, Q. S. *Phys. Rev. Lett.* **1999**, *83*, 3001−3004.
(33) Zeng, C. G.; Li, B.; Wang, B.; Wang, H. Q.; Wang, K. D.; Yang, J. L.; Hou, J. G.; Zhu, Q. S. *J. Chem. Phys.* **2002**, *117*, 851−856.
(34) Li, B.; Zeng, C. G.; Li, Q. X.; Wang, B.; Yuan, L. F.; Wang, H. Q.; Yang, J. L.; Hou, J. G.; Zhu, Q. S. *J. Phys. Chem. B* **2003**, *107*, 972−984.
(35) Tersoff, J.; Hamann, D. R. *Phys. Rev. B* **1985**, *31*, 805−813.
(36) Tersoff, J.; Hamann, D. R. *Phys. Rev. Lett.* **1983**, *50*, 1998−2001.

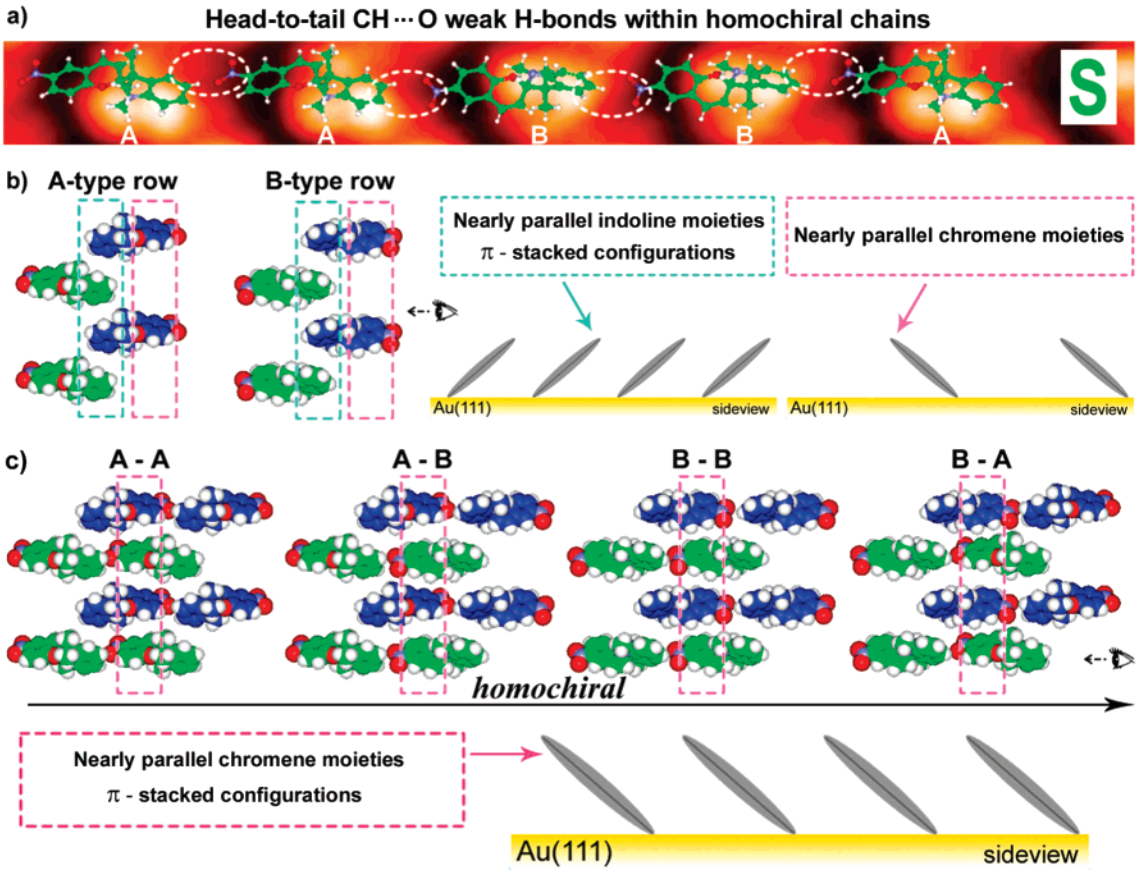

Figure 7. (a) An (S)-SP6 homochiral chain with superposed molecular models. Dashed ellipses indicate the potential C−H···O weak H-bonds between adjacent SP6. The STM image is extracted from Figure 2a. (b) CPK packing models of A- and B-type rows. The side view schematic drawing shows the π-stacking of the indoline moieties (green dashed frame) and the nearly parallel packing of the chrosmene moieties (pink dashed frame) within a single row. (c) CPK packing models of the combining configurations corresponding to the experimental observations. The side view schematic drawing shows the π-stacking of the chromene moieties of SP6 molecules between adjacent rows (pink dashed frame). All these four configurations preserve the homochirality along the direction perpendicular to the rows.

"point-out" adsorption orientation. In both of the "point-in" and "point-out" orientations, the two orthogonal near-planar heterocyclic fused rings of the SP6 molecule resemble an "X" shape in the side view. The top and the side views of the adsorption configurations can be found in the Supporting Information (Figure S1). By matching the simulated STM patterns with the experimental ones, we also obtain the packing models of A- and B-type rows. Within each row SP6 molecules with opposite chirality pack alternately, arrange their long axis perpendicular to the row, attach to the Au(111) surface with the same function groups, and expose the same parts to be imaged, as shown in Figure 3b. Therefore each two neighboring molecules within an SP6 row display enantiomorphous shapes in the STM images. The chromene moieties of adjacent rows (A- or B-type) interdigitate into the clefts of each other to form the close packed 2D structure. Figure 5 shows the STM image obtained under accidental, special tip conditions, where the geometric shapes of SP molecules are rendered. Each SP6 molecule appears as a *pollywog* with a length of ∼1.3 nm and arranges the long axis perpendicular to the rows. Adjacent rows join together just like *zippers* to form the close packed 2D structure. These observations strongly support the *flat-lying* adsorption configurations and the interdigitated arrangements of the SP6 molecules within the 2D domain as we proposed in Figure 3b.

It is interesting to notice that in the area shown in Figure 2a the parallel rows take a relatively disordered A/A/B/B/A/B/B arrangement from left to right instead of the conventional alternate arrangement. However, by identifying the absolute chirality of each SP6 molecule, we surprisingly find a quasi chiral separation in this 2D orientationally disordered domain; the 2D domain separates into homochiral chains running along the direction perpendicular to the rows (Figure 6a). Further observations on more samples reveal that both the orientational disorder and the quasi chiral separation are the common characteristics of the 2D SP6/Au(111) systems (Figure 6b−d).[38] To our knowledge, this is the first example showing the spontaneous chiral resolution in a 2D orientationally disordered system.

In order to gain insight into the origin of this unique phenomenon (chiral order in orientationally disorderd system), we list in Figure 7 an (S)-SP6 homochiral chain with the superposed molecular models which shows the head-to-tail coupling of the SP6 molecules within the chain. Although SP6 does not have functional groups which can form strong hydrogen

(37) Here "same adsorption orientation" only means the same orientation relative to the Au surface plane while the azimuthal orientations of (S)- and (R)-SP6 molecules are different.

(38) Up to 20 samples prepared under the same conditions have been examined, and for each sample more than 10 positions were randomly observed to achieve a statistically significant result.

bonds (H-bonds), the $-NO_2$ of one molecule and the hydrogen of the phenyl from an adjacent molecule may provide C−H···O weak hydrogen bonds (H-bonds). Such attractive interactions have been demonstrated to be significant in the formation of chiral clusters and the chiral phase transition of 1-nitronaphthalene molecules on Au(111) surfaces.[12] Analogous C−H···O weak H-bonds were also considered to be responsible for chiral recognition of PVBA molecules on a Cu(100) surface.[11] Hence the *head-to-tail* coupling of the SP6 molecules within each homochiral chain is thought to be associated with these attractive C−H···O weak H-bonds.

As we mentioned before, orthogonal chromene and indoline rings of each SP6 molecule are both tilted from the normal of the surface and resemble an "X" shape in the side view. Within each A- (or B)-type row, the nearly parallel indoline moieties are tilted toward almost the same direction and have the well-known π-stacked configurations (Figure 7b).[39−41] Since the chromene and the indoline rings are orthogonal in each SP6, the chromene rings of SP6 within each row also have nearly parallel packing but are tilted toward another direction (Figure 7b). Despite the various A/B distributions in the 2D SP6 domains, we only observed four particular combining configurations between adjacent rows which preserve the homochirality along the direction perpendicular to the rows (Figure 7c). In all these configurations, the chromene rings from adjacent rows also have nearly parallel packing; i.e., the chromene moieties also have the π-stacked configurations. Thus all the 2D domains have the same kind of densely packed structure which allows the π-stacking of both the chromene moieties from adjacent rows and the indoline moieties within each row.

Integrating two neighboring SP6 rows (A- or B-type) with the close packed positional order will result in up to 10 different combining configurations.[42] Besides four experimentally observed combining configurations which preserve the homochirality along the direction perpendicular to the rows (Figure 7c), there are also six possible configurations which will result in the heterochirality along this direction (Supporting Information, Figure S3). Different from the configurations shown in Figure 7c, in all six of these configurations, the chromene moieties from adjacent rows pack crosswise. Although these six configurations are also feasible for the formation of the (aromatic) C−H···O (of nitro group) weak H-bonds, the absence of them in the experiments implies these six configurations compared to the configurations shown in Figure 7c are less energetically stable. Hence we conclude that the π-stacking of the chromene moieties along the rows is also crucial for the quasi chiral phase separation of the 2D domains. In conclusion, the SP6 moelcules form structures which allow the C−H···O weak bonds as well as the π-stacking of two orthogonal aromatic rings of each SP6 and, consequently, undergo the unique quasi chiral separation in the 2D orientationally disordered domains.

Conclusion

In summary, we have observed a quasi chiral separation in 2D orientationally disordered 2D SP6/Au(111) systems. The 2D domains separate into 1D homochiral chains in which the SP6 molecules adopt two possible orientations randomly. Our finding demonstrates that the chiral separation can occur in relatively complex 2D systems and provides the possibility to obtain 1D homochiral molecular structures with different exposed functional groups on solid surfaces. These novel structures may have potential applications in multicomponent chiral sensing and multistep enantioselective catalysis.

Acknowledgment. This work was supported by the National Basic Research Program of China (2006CB922001) , by the National Natural Science Foundation of China (50121202, 50532040, 10474088, 10374083, 20573099), by the USTC-HP HPC project, and by the Virtual Laboratory for Computational Chemistry of CNIC and Supercomputing Center of CNIC, Chinese Academy of Sciences.

Supporting Information Available: Computational methodology, top and side view models of (S)- and (R)-SP6 adsorbed on Au(111) surface, determination of the ten possible combining configurations, packing models of experimentally unobserved combining configurations. This material is available free of charge via the Internet at http://pubs.acs.org.

JA066521P

(39) Zhou, Y. S.; Wang, B.; Zhu, M. Z.; Hou, J. G. *Chem. Phys. Lett.* **2005**, *403*, 140−145.
(40) Kwon, K. Y.; Lin, X.; Pawin, G.; Wong, K.; Bartels, L. *Langmuir* **2006**, *22*, 857−859.
(41) Dou R. F.; Ma, X. C.; Xi, L.; Yip, H. L.; Wong, K. Y.; Lau, W. M.; Jia, J. F.; Xue, Q. K.; Yang, W. S.; Ma, H.; Jen, A. K. Y. *Langmuir* **2006**, *22*, 3049−3056.

(42) Considering neither A- nor B-type rows have C_2 symmetry, the configurations are the combinations of four building blocks: *A*, $\bar{A}$, *B*, and $\bar{B}$. Here $\bar{A}$ ($\bar{B}$) indicates the configuration obtained by rotating *A*(*B*) 180° in the paper plane. There are 16 combinations in total: *AA*, *AB*, $A\bar{A}$, $A\bar{B}$, *BA*, *BB*, $B\bar{A}$, $B\bar{B}$, $\bar{A}A$, $\bar{A}B$, $\bar{A}\bar{A}$, $\bar{A}\bar{B}$, $\bar{B}A$, $\bar{B}B$, $\bar{B}\bar{A}$, and $\bar{B}\bar{B}$. However, some of them (*AA* and $\bar{A}\bar{A}$, *AB* and $\bar{B}A$, *BA* and $\bar{A}B$, *BB* and $\bar{B}\bar{B}$, *AB* and $\bar{B}A$, *AB* and $\bar{B}A$) are equivalent since the arrangements of the SP6 molecules in these configurations are identical. Therefore there are only 10 different combining configurations. The detailed discussion can be found in the Supporting Information (Figure S2).